Deep Excavations in Taipei Metro Construction

R. N. Hwang[1] and Z. C. Moh[2]
Moh and Associates, Inc., New Taipei City, Taiwan, Republic of China
[1]*E-mail: richard.hwang@maaconsultants.com*

ABSTRACT: Discussed herein are the geological features of the Taipei Basin relevant to the construction of Taipei Metro and the deep excavations carried out with emphasis on back analyses of wall deflections. The excavation at the crossover next to G17 Station of the Green Line is adopted as an example to illustrate the applications of wall deflection paths and reference envelopes. The importance of calibrating inclinometer readings to account for the movements at the tips is confirmed by numerical analyses; and the assumption that movements at the joints between the struts at the first level and the diaphragm walls would be negligible in subsequent stages of excavation once these struts are preloaded is verified. Furthermore, it is proved that the concept of wall deflection path is very useful to quantify the influence of various factors, e.g., the depth and width of excavation, wall length, preloads of struts, and the thickness of soft deposits, on the performance of diaphragm walls.

KEYWORDS: Taipei Basin, Underground Construction, Deep Excavation, Dewatering, Wall Deflection Path, Reference Envelope

1. INTRODUCTION

The Department of Rapid Transit Systems (DORTS) of Taipei City Government was inaugurated in June, 1986 and the construction of Taipei Metro commenced in December, 1988. As depicted in Figure 1, as of this date (June, 2016), there are 5 lines, with a total of 117 stations and a route length of 136.7 km, in revenue services. With a daily patronage of, on an average, 2.1 million, this metro system effectively eases the traffic congestion in the city and has become the most favoured mode of transportation for the residents.

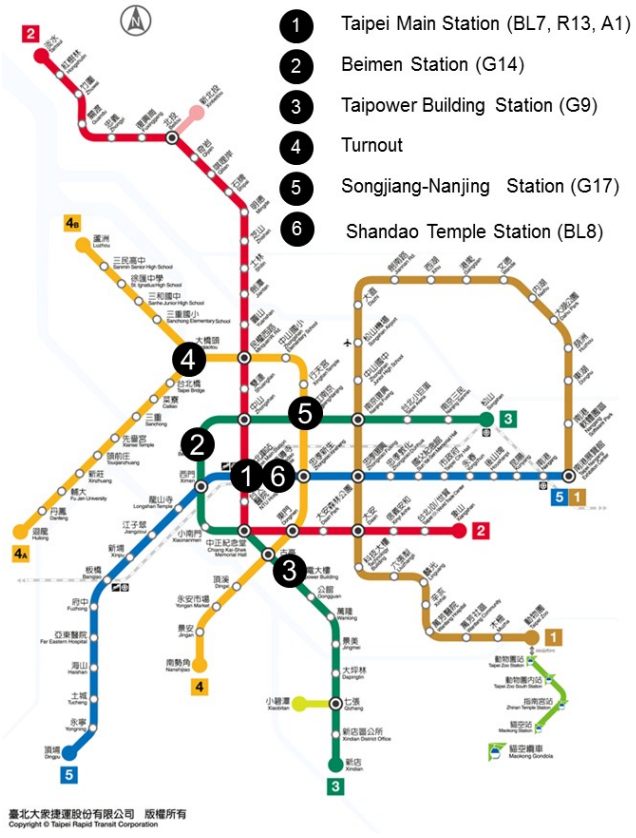

Figure 1 System map of as of June 2016

The underground constructions of the metro system, mainly consisting of cut-and-cover constructions and tunneling, have been great challenges to geotechnical engineers and have led to drastic advancement of technology of the construction industry. Because of the presence of a water-rich gravely layer, i.e., the Jingmei Formation, underlying the soft deposits, i.e., the Songshan Formation, failures occurred frequently in the Stage 1 constructions carried out in the 1990's for the so-called Priority Network. As more experience gained and as rigid risk management policies are enforced, no severe accidents occurred since 2000.

Discussed herein are the deep excavations carried out for constructing the metro facilities with the results of back analyses performed for establishing soil parameters for future designs.

2. GEOLOGY OF THE TAIPEI BASIN

The Taipei Basin, refer to Figures 2 and 3, was formed as a result of ground subsidence due to tectonic movements in the Middle Pleistocene Epoch. The Central Geological Survey (CGS) of the Ministry of Economic Affairs has conducted extensive studies to reveal the geology in the basin. As can be noted from the schematic profile shown in Figure 3, which was prepared based on the information collected from the deep holes sunk by CGS, the sediments in the basin include, from top to bottom, the Songshan (or, Sungshan as previously translated) Formation, Jingmei (or, Chingmei) Formation, Wugu Formation and the Banqiao (or, Panchiao) Formation (Teng, et al. 1999; 2004). The deepest depth to the base formation, i.e., the deformed Tertiary Strata, is 679m.

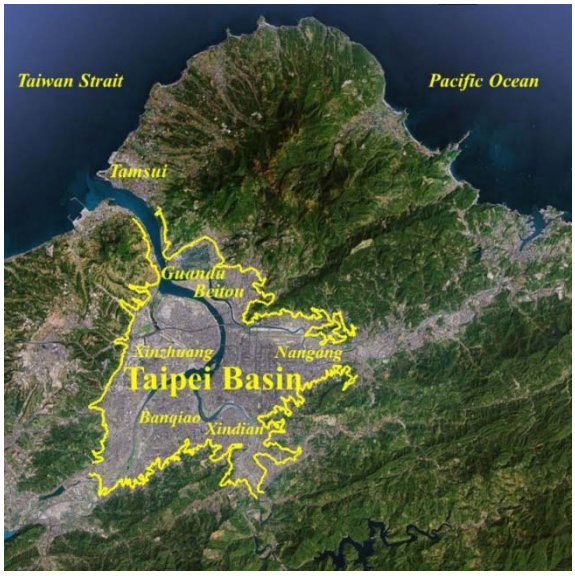

Figure 2 Satellite Image of the Taipei Basin

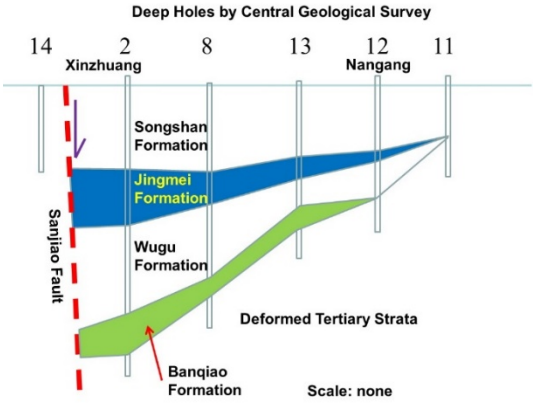

Figure 3 Schematic geological profile of the Taipei Basin

2.1 The Songshan Formation

Figure 4 shows a geological map (Lee 1996) of the Taipei Basin which was formed by deposition of sediments from the Danshui (or Tamsui as previously translated) River and her three tributaries, namely, the Jilong (or Keelung) River, Xindian (or Hsientien) Creek and Dahan (or Tahan) Creek. Geological zoning was thus conducted accordingly and geological zones were designated as, e.g., T1 and T2 along the Dahan Creek, K1 and K2 along the Jilong River and H1 and H2 along the Xindian Creek.

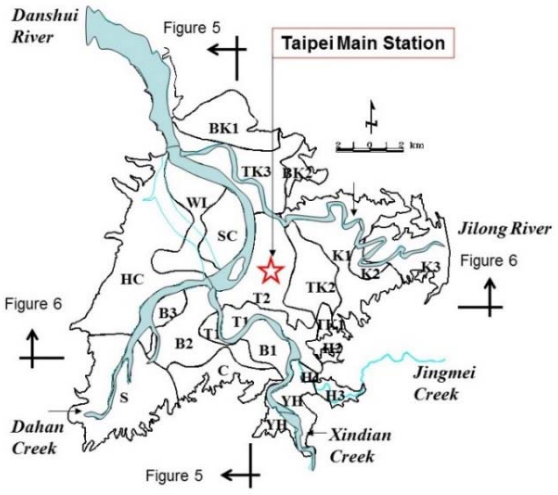

Figure 4 Geological map of the Taipei Basin (Lee, 1996)

Figure 5 shows a north-south geological profile between Beitou and Xindian (refer to Figure 2 for locations) and Figure 6 shows an east-west geological profile between Nangang and Banqiao of the Taipei Basin. As can be noted, the Jingmei Formation exists at depths varying from 40m to 70m in the central city area in which Taipei Main Station (Location 1 in Figure 1) is located. Figure 7 shows the results of a piezocone penetration test carried out at Shandao Temple Station (BL8) which is the next station in Line 5 (the Blue Line) to the east of Taipei Main Station (BL7), i.e., Location 6 in Figure 1. The typical 6-layer sequence of subsoils in the Songshan Formation is clearly identifiable from the profiles shown, particularly the profile for pore pressure response. Layers I, III and V consist of mainly silty sands (Soil Type SM) and Layers II, IV and VI consist of mainly silty clays (Soil Type CL). As depicted in Figure 6, toward the west, the stratigraphy becomes more complicated with sandy and clayey seams frequently interbedded in the major layers; and toward the east, the sandy layers diminish and clays become dominating. Similarly, clays become dominating toward the north of the basin as depicted in Figure 5.

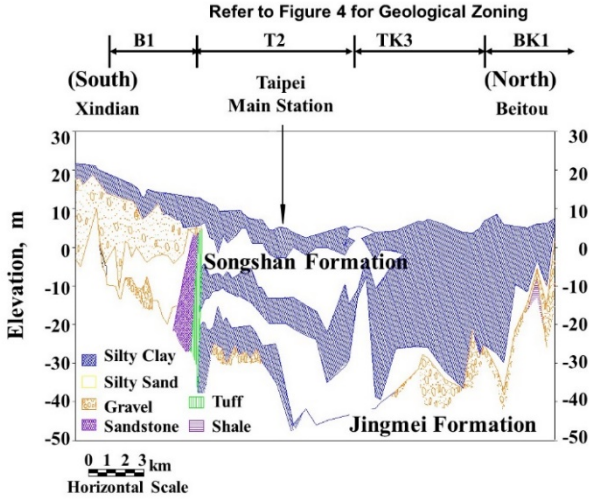

Figure 5 North-South geological profile of the Taipei Basin

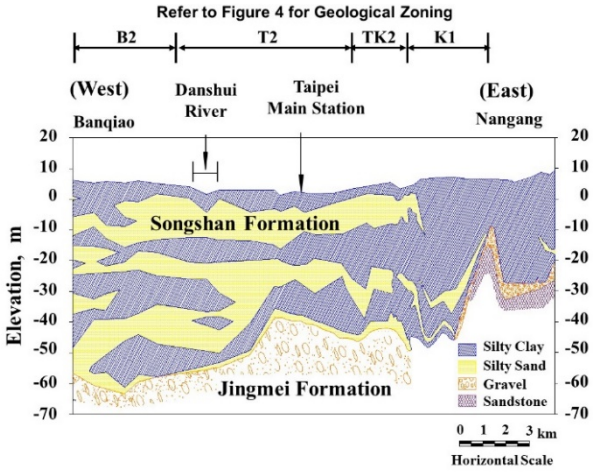

Figure 6 East-West geological profile of the Taipei Basin

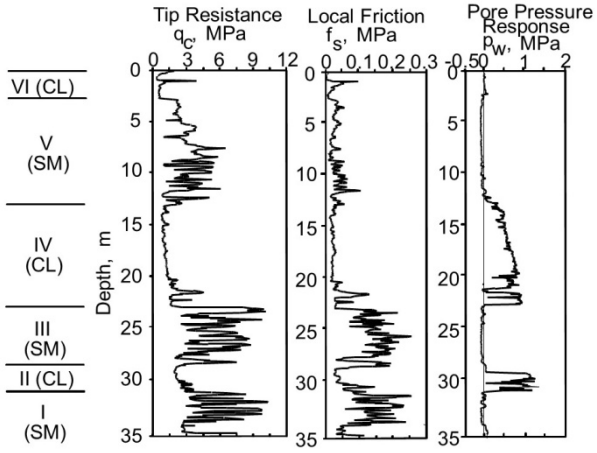

Figure 7 Results of piezocone penetration tests at Shandao Temple Station

The properties of the sublayers in the Songshan Formation have been well discussed in literatures (Moh and Ou 1979; MAA 1987; MAA Group 2007). The lowering of piezometric level in the underlying Jingmei Formation, as to be discussed in Section 2.2, has

led to significant reductions of water pressures in the Songshan Formation, and, as a result, ground has settled by more than 2m at Beimen Class 1 Reference Point near Beimen Station (Location 2 in Figure 1) as shown in Figure 8. Based on the long-term records depicted in Figure 9, the piezometric level in Layer III in the central city area, where Taipei Main Station is, is estimated to be as low as EL-27m in the 1970's. This level is about the same as the bottom level of Layer III, or even lower. In other words, the porewater pressure in Layer III was practically nil then. This is confirmed by Figure 10 which shows the changes of piezometric levels in various layers in the past.

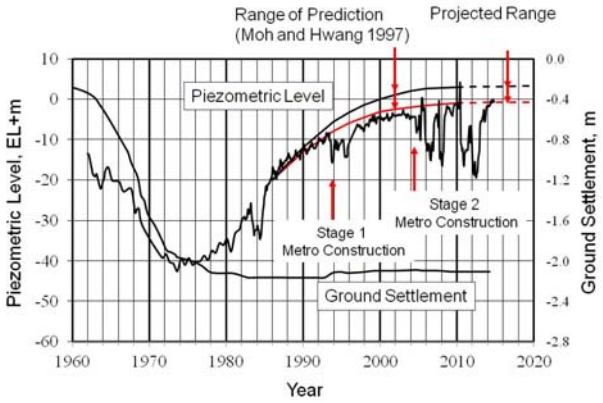

Figure 8 Piezometric level in the Jingmei Formation and ground settlement at Beimen Class 1 Reference Point near Beimen Station

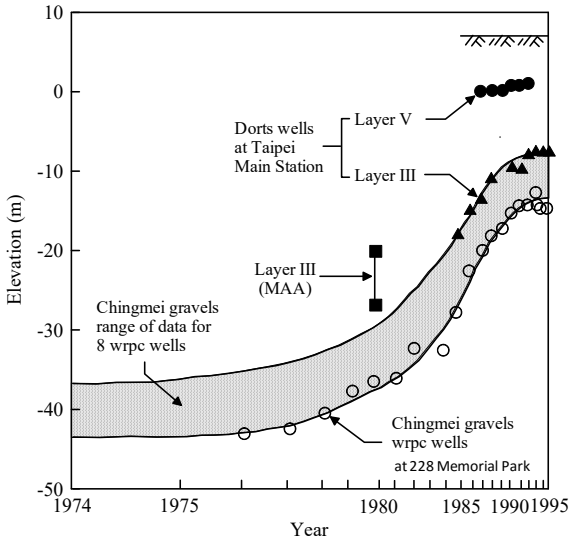

Figure 9 Drawdown of groundwater in the Songshan Formation in the central area of Taipei City (after Chin 1997)

Regarding the piezometric level in Layer V, little information is available for estimating its lowest value. The underlying Layer IV is sufficiently thick to cut off the cross flow from Layer V to Layer III. It is thus reasonable to assume that the piezometric level in Layer V was unaffected by pumping of water from the Jingmei Formation. An extensive research program was conducted in 1979 and continued for 3 years to monitor the fluctuations of groundwater and the results indicated that the piezometric level in Layer V varied from EL+1.5 to EL-1.0m in the central city area (Ou el al. 1983). On the other hand, since the overlying Layer VI is thin, or even absent at places, Layer V is constantly recharged by surface runoff and the piezometric levels in Layer V are primarily affected by the fluctuations of water level in the rivers. It has been noticed that pumping for lowering water pressures for maintaining stability and/or for drawing water as a supply to construction activities during excavations also affected the groundwater levels in shallow layers. But such influence was quite localized and temporary. For practical purposes, the piezometric level in Layer V can be assumed at a low of EL-1m and at a high of EL+2m.

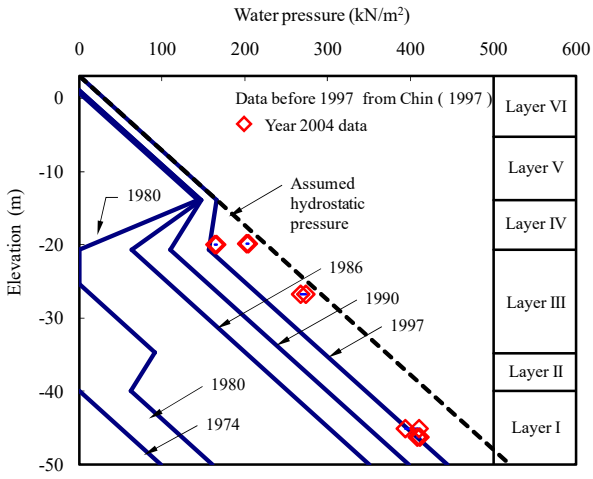

Figure 10 Changes in groundwater pressures in the Songshan Formation in central area of Taipei City (after MAA Group 2007)

Due to the reduction of porewater pressures, all the subsoils in the Songshan Formation in the central city area have been substantially over-consolidated. This is particularly true for Layer II because the underlying Layer I is very permeable and the piezometric level in Sublayer I was practically the same as the piezometric level in the Jingmei Formation. The undrained shearing strengths of the clays were extensively studied by the Geotechnical Engineering Specialty Consultant engaged by the DORTS as a designated task at the beginning of metro construction in 1991. Laboratory tests were carried out in collaboration with the soil laboratory of Massachusetts Institute of Technology. Figure 11 shows the results obtained (Chin et al. 1994; Hu et al. 1996; Chin & Liu 1997).

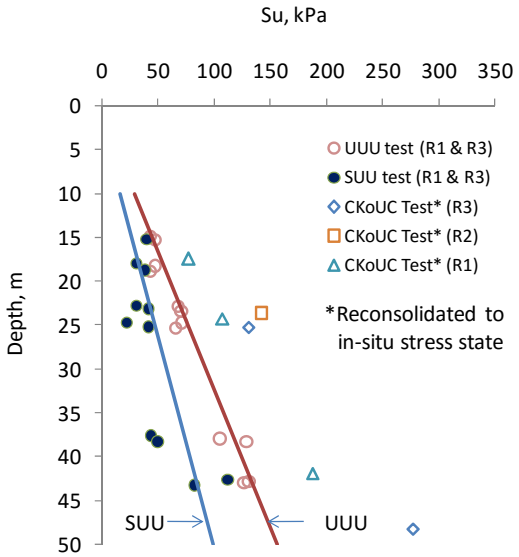

Figure 11 Comparison of undrained strengths from various types of tests (modified from Chin et al. 1994)

Based on these results, Hwang et al. (2013) studied the consolidation effects at Taipei Main Station and Taipower Building (Location 3 in Figure 1) and proposed Figure 12 for estimating the Ko-consolidated-undrained compression (CKoUC) strengths, i.e., the so-called SHANSEP strengths (Ladd and Foott 1974), of clays in the

T2, TK2 and K1 zones. Table 1 shows the CkoUC, Ko-consolidated-undrained-extension (CkoUE) and direct-simple-shear (DSS) strengths of soils in Layers II and IV at the location of Taipei Main Station. The set of results for 1990 is in good agreement with those obtained from CKoUC tests as depicted in Figure 12 but are considerably greater than those obtained in the saturated-unconsolidated-undrained (SUU) and unsaturated-unconsolidated-undrained (UUU) tests shown in Figure 11. The shear strength at a depth of, for example, 40m is about 200 kPa while Figure 11 shows a value of about 80 kPa for SUU tests and 120 kPa for UUU tests. As can be noted from Table 1, the shear strengths were reduced by, up to, 10% as a result of recovery of piezometric levels from 1974 to 1990.

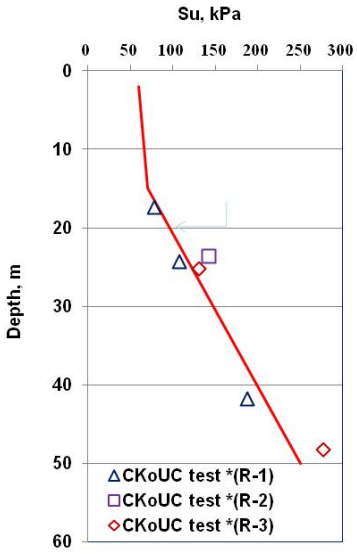

Figure 12 Estimated undrained shear strengths of clays in T2, TK2 and K1 Zones in 1990 obtained by CKoUC tests (Hwang et al. 2013)

Table 1 Estimated undrained strengths of clays at Taipei Main Station (Hwang et al. 2013)

Layer	Depth	Estimated Undrained Shear Strength, kPa					
		Year 1974			Year 1990		
		CKoUC	CKoUE	DSS	CKoUC	CKoUE	DSS
IV	16.3m	38	22	27	36	21	25
	23.3m	117	69	84	111	66	78
II	32.3m	174	103	125	161	96	113
	47.3m	258	153	185	238	142	166

2.2 The Jingmei formation

From an engineering point of view, the formation of the most interest is the Jingmei Formation which is sometimes referred to as Jingmei Gravel. First of all, it is a bearing stratum for deep foundations. Secondly, it was responsible for several disastrous events in the early stage of metro construction (Moh, et al., 1997; Hwang, et al., 1998). Because it is extremely permeable and water-rich, once water from the gravel finds its way to suddenly discharge into a pit, it is nearly impossible to stop the flow. Most of the disasters occurred during launching of shield machines at launching shafts or during arrival of shield machines at reception shafts (Lin, et al., 1997). In another scenario, water suddenly discharged into a station excavation as a hole was made through the overlying Songshan Formation to replace a malfunctioning piezometer installed in the Jingmei Formation. It became necessary to flood the whole pit by breaking a water main to discharge water into the pit to balance the groundwater pressure and stop the flow. It was estimated that 70,000 cubic meters of water was discharged into the pit in 18 hours (Moh, et al., 1997). The presence of this water-bearing aquifer makes the geology of the Taipei Basin unique and challenging to geotechnical engineers.

The Jingmei Formation, which is composed mainly of cobbles and boulders embedded in matrices of sandy gravels, is an alluvial fan formed by the deposits transported by the Xindian Creek, refer to Figure 4, from the south. Teng et al. (1994; 2004) reported that the Jingmei Formation has a maximum thickness of 60m near Xinzhuang (Location 2 in Figure 13) and diminishes around the perimeter of the Taipei Basin. The top of this alluvial fan dips toward northwest and has the lowest elevation of 120 m below sea level at Wugu (Location 6 in Figure 13). The Jingmei Formation is a water-rich aquifer and was once the sole source of water supply of the city. The piezometric level of groundwater in the Jingmei formation was a few meters above the ground level at the turn of the 20th century (Wu, 1968) and dropped drastically as a result of excessive pumping. It was closely monitored by Water Resources Planning Commission (WRPC) before it merged into Water Resource Bureau (WRB) in 1996. Water Resource Bureau later merged into Water Resources Agency (WRA) in 2002 and the monitoring has been continuing ever since. Figure 8 shows the variation of piezometric level of groundwater in the Jingmei Formation and ground settlement observed at Beimen (meaning North Gate in Chinese) near Beimen Station, refer to Figure 1 for location. As can be noted, the piezometric level dropped to, as low as, EL- 40m, which corresponds to a depth of 44m (ground level = EL+4m) in the 1970's. Because the Jingmei Formation is extremely permeable, the groundwater drawdown was widely spreading. As can be noted from the contours showing in Figure 13, the drawdown in the Jingmei Formation in year 1975 was the largest in Xinzhuang and significant drawdown extended all the way to the rim of the basin (WRPC 1976).

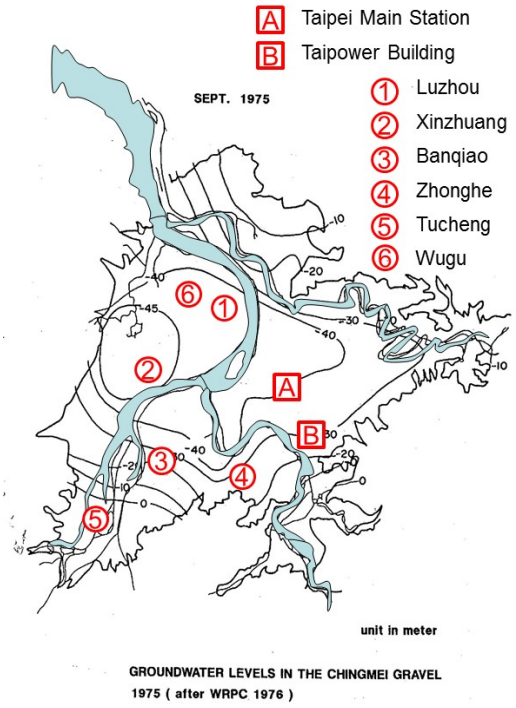

Figure 13 Contour of groundwater drawdown in the Jingmei Formation in 1975 (after WRPC 1976)

Alerted by the significant ground subsidence, the government started to regulate pumping of groundwater in 1968 and the piezometric levels became steady in the 1970's. As depicted in Figure 8, the piezometric levels started to rise in the early 1980's as surface runoff gradually replaced groundwater as the source of water supply. The recovery, however, has been slowed down since the early 1990's due to the lowering of groundwater pressures for maintaining

the stability of deep excavations in several large infrastructure projects, particularly, the metro systems. The drawdown at Beimen (North Gate) was much larger in Stage 2 metro construction in 2000's than that in Stage 1 construction in the 1990's as several large scale dewatering schemes were carried out in the neighbourhood, for examples, G14 Station of the Green Line of Taipei Metro and Taipei Main Station (A1 Station) of Taoyuan International Airport Access MRT. As major constructions in the central city area were all completed by 2014, the piezometric level in the Jingmei Formation quickly recovered to EL. +0m which falls on the lower bound of the prediction projected from the previous prediction made in Moh and Hwang (1997). Whether it will rise further remains to be observed. Based on the readings obtained so far, it is envisaged that the piezometric level in the Jingmei Formation in the central city area is unlikely to exceed EL+3m in the coming years. However, it did reach EL+4.03In July 2010 as depicted in Figure 8. Since readings were taken monthly, it is unsure whether these readings were caused by abnormal events.

The disastrous incidents experienced in Stage 1 constructions of Taipei Metro back in the 1990's can be attributed to the facts that, firstly, the excavations were unprecedented at that time, as previous excavations were mostly for basements of less than 15m in depth while the depths of metro excavations generally range from 20m to 30m, and secondly, the piezometric level in the Jingmei Formation had risen by 30m from its lowest level during the 1970's. With the experience gained in the Stage 1 constructions, designers and contractors were much more cautious in dealing with groundwater problems and no serious failure occurred in Stage 2 constructions of Taipei Metro in the 2000s.

3. DEEP EXCAVATIONS IN TAIPEI METRO

Excavations seldom exceeded 30m in depth in the old days for various reasons but, with increasing demand for underground spaces and with advanced construction technology, excavations exceeding this depth are very common nowadays. This is particularly true for metro constructions. For example, in Taipei Metro, as depicted in Table 2, there were 9 sites at which the excavation exceeded 30m. It is therefore desirable to re-define deep excavations to comply with the state-of-the-practice. Hwang et al. (2006) proposed to classify excavations into 5 categories, from shallow to extremely deep, as depicted in Table 3.

Table 2 Deepest excavations in Taipei Metro construction

Site	Metro Line	Depth
Jingan Station (O18)	Line 4: Zhonghe-Xinlu Line	30.23m
Dongmen Station (R10/O14)	Line 2: Danshui-Xinyi	31.20m
Daqiaotou Station (O8)	Line 4: Zhonghe-Xinlu	32.00m
Beimen Station (G14)	Line 3: Songshan-Xindian	32.10m
Taipei Bridge Station (O7)	Line 4: Zhonghe-Xinlu	33.00m
Ventilation Shaft B	Line 5: Bannan Line	33.81m
Ventilation Shaft	Line 4: Zhonghe-Xinlu Line	34.95m
Ventilation Shaft A	Line 5: Bannan Line	36.60m
Turnout	Line 4: Zhonghe-Xinlu	40.00m

Table 3 Classification of excavations (Hwang et al. 2006)

	Shallow	Median	Deep	Very Deep	Extremely Deep
Depth	<5m	5-10m	10-20m	20-30m	>30m
Basement Nos	1	2-3	4-5	6-7	>7
Metro Station Levels			2	3-4	>5

3.1 Deepest Excavation

Figure 14 shows the deepest excavation carried out in the Taipei Basin. It was carried out to a depth of 40m at the west bank of the Danshui River for constructing a turnout (Location 4 in Figure 1) in the Zhonghe-Xinliu Line (Line 4) in Stage 2 metro construction. The pit was retained by diaphragm walls of 1.5m in thickness and 63m in length. Because of the absence of a continuous clayey layer below the formation level, it was necessary to form an impervious slab at the toe level of the diaphragm walls to seal off seepage and to resist water pressures at the bottom. This slab was installed by using high-pressure jet grouting. Even with this grouted slab, pumping was still required to lower the piezometric pressures in the Jingmei Gravel by 13m or so for maintaining a sufficient factor of safety against uplift. The entire turnout is 126m long and was partitioned into 5 sections by internal diaphragm walls. Excavations were carried out, from the east toward the west, section by section. This reduced the maximum pumping rate to 3000 m^3/hour (DORTS 2010).

The excavation for the turnout was carried out in 2005. The piezometric level in the Jingmei Formation had risen to EL-3m by then. If the excavation were carried out in the 1980's when the piezometric level was at, roughly, EL-16m, dewatering would not have been necessary. Furthermore, if the excavation were carried out in the 1970's, even the grouted slab would not have been necessary.

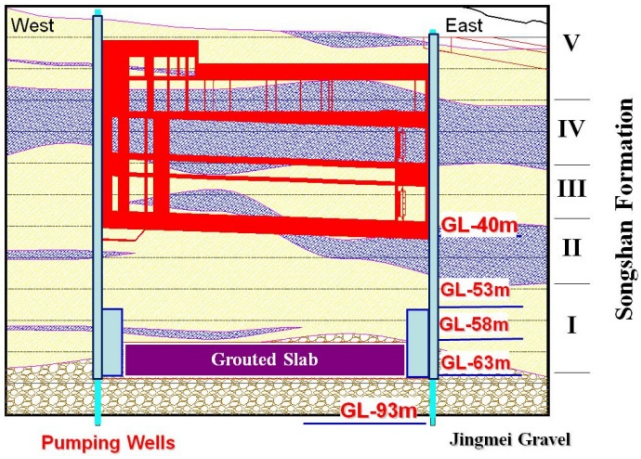

Figure 14 Excavation carried out at the Turnout

3.2 Largest Dewatering Scheme

Dewatering was necessary for all the deep excavations listed in Table 2. The largest dewatering scheme was carried out in 2012 for constructing the Taipei Main Station (A1 Station, Location 1 in Figure 1) of Taoyuan International Airport Access MRT; and the pumping rate of 7,000 m^3/hour is the record high in the Taipei Basin and could well be the record high for the entire island (Moh and Hwang 2015). Prior to that, pumping with a similar rate (6,564 m^3/hour maximum) was carried out in 2007 at Taipei Bus Station across Civic Boulevard to the north of Taipei Main Station.

As discussed in Section 2.1, the lowering of the porewater pressures in the Songshan Formation as a result of drawdown of the piezometric level in the Jingmei Formation has increased the undrained shearing strengths and reduced the compressibility of the clays. Subsequent deep excavations have been benefited as lighter retaining structures can be used; and, furthermore, dewatering at the sites with large pumping rates did not lead to intolerable ground settlements in areas with previous consolidation settlements.

4. BACK ANALYSES – CASE STUDY

Ground settlement which is one of the primary factors affecting the structures in adjacent to excavations is closely related to the maximum wall deflections. The maximum wall deflections thus become the most important subject in evaluating the performance of diaphragm walls.

Wall deflections are routinely monitored by using inclinometers. The readings obtained are inevitably affected by the movements at the tips which are assumed to be fixed and wall deflections at other

depths are calculated accordingly. Hwang et al. (2007b) recommended to calibrate inclinometer readings by assuming that the joints between the struts at the first level and the diaphragm walls would not move once these struts are preloaded. This recommendation was based on the finding that the changes in the lengths of these struts would be minimal as the load increments and/or decrements in the struts would be small. To illustrate this point, the readings obtained in the cut-and-cover construction for the crossover, refer to Figure 15, next to G17 Station (Sonjiang Nanjing Station (Location 5 in Figure 1) of Line 3 (the Green Line) of Taipei Metro are discussed herein. The excavation was carried out to depths varying from 17.7m to 20.2m below the ground level (at EL+4m) in 7 stages as depicted in Figure 16 and the pit was retained by diaphragm walls of 1m in thickness and braced by steel struts at 6 levels.

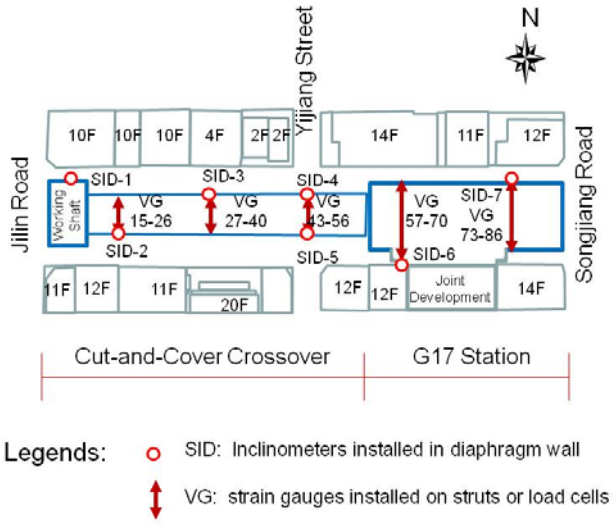

Figure 15 Layout of G17 Station of the Green Line of Taipei Metro and the cut-and-cover crossover

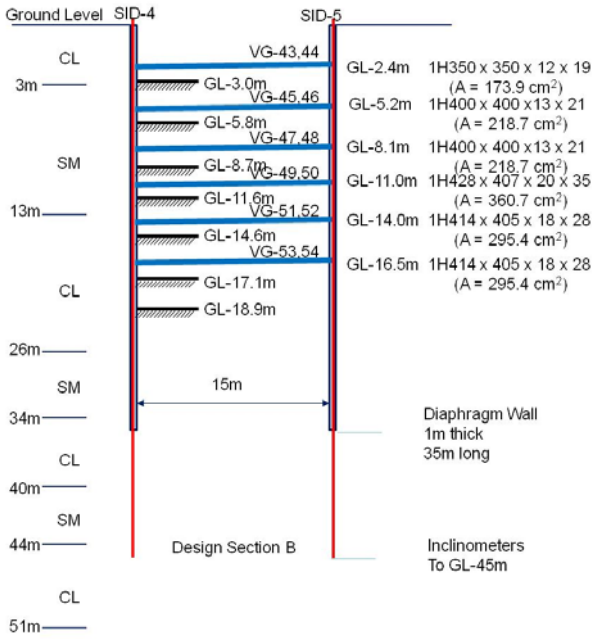

Figure 16 Excavation scheme for the crossover next to G17 Station

4.1 Calibration of Inclinometer Readings

Figure 17 shows the strut loads recorded by two strain gauges, namely, VG-43 and VG-44, installed on the first level strut between Inclinometers SID-4 and SID-5. As can be noted, the strut was preloaded to 71 tones, which is the average of the readings of the two gauges, at the beginning. The load in the strut increased to 87 tons in the second stage of excavation and dropped to a minimum of -3 tons in the subsequent stages. For a strut length of 14m and an Young's Modulus, i.e. the E-value, of 200,000 N/mm^{2,} the increment of 16 tones, i.e., from 71 tons to 87 tons, corresponds to a shortening of 0.6mm of the strut or an inward movement of 0.3mm at each end; and the decrement of 74 tons, i.e., from 71 tons to -3 tons, corresponds to a lengthening of 3mm of the strut or an outward movement of 1.5mm at each end. Movements of such magnitudes are negligible for practical purposes and the joints between the struts and the diaphragm walls can indeed be assumed fixed for calibrating the readings at other depths.

Ideally, the changes in the length of the strut can be confirmed by studying the relative movements between Inclinometers SID-4 and SID-5. In fact, this was exactly the purpose to install inclinometers at the two ends of the strut. However, as illustrated above, the fact that the inclinometer readings are affected by the movements at the tips totally defeats the purpose.

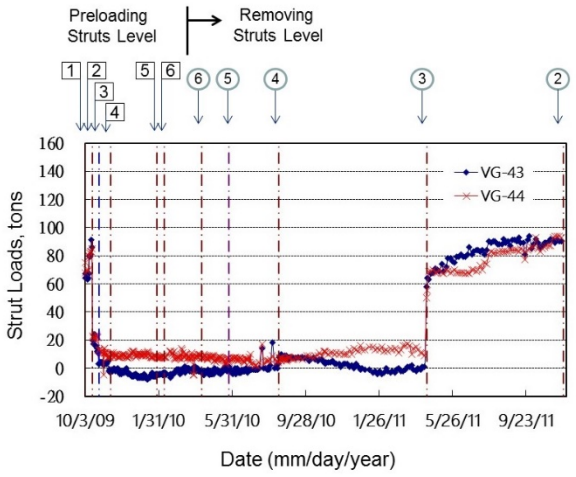

Figure 17 Loads in the 1st level strut between SID-4 and SID-5

The final readings of the 4 inclinometers, duly calibrated, in the diaphragm walls retaining the excavation of the crossover are shown in Figure 18. A maximum wall deflection of 34.1mm was obtained at the location of SID-2 and a maximum of 35.6mm was obtained at the location of SID-3. It is interesting to note that the diaphragm wall toe moved by 16.4mm, 18.8mm, 14.8mm and 13.6mm at the locations of SID-2, SID-3, SID4 and SID5, respectively, estimated based on the assumption that the wall at the first strut level would not move once the struts were preloaded. It has become quite common nowadays to install inclinometers in diaphragm walls and stop at the toe levels of the diaphragm walls to save the costs. The toe movements of these magnitudes were, nearly, 50% of the maximum wall deflections for the case studied and analyses would certainly lead to misleading conclusions if inclinometer readings were not corrected. It can also be noted from Figure 18, the tips of the inclinometers still moved by, as much as, 10mm, or 25% of the maximum wall deflections, even with a 10m extension below the toes of the diaphragm wall.

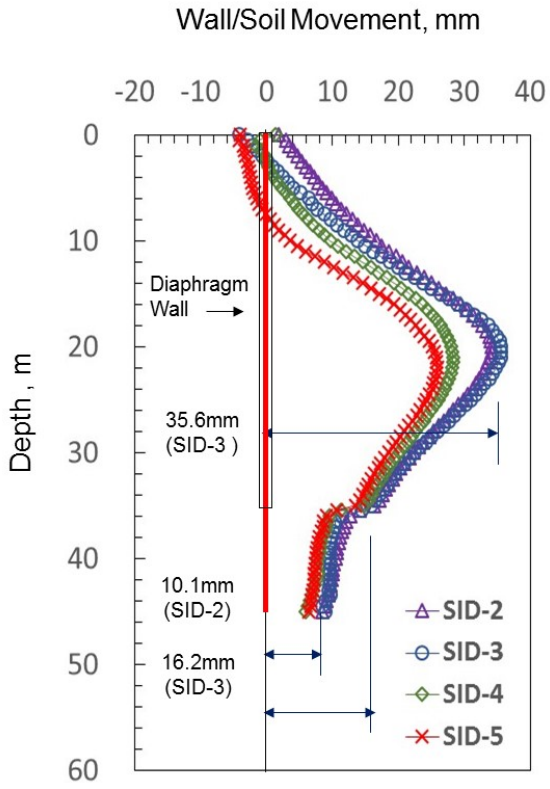

Figure 18 Final wall deflections at the end of excavation

4.2 Numerical Analyses

Numerical analyses were conducted by using the two-dimensional finite element computer program PLAXIS (PLAXIS BV 2011). Figure 19 shows the finite element model adopted. The soil parameters suggested by the Detailed Design Consultant of the project are given in Table 4 (MAA 2005). The Young's moduli, E', were correlated to soil strengths by using the following empirical relationships:

$$E' = 500\ S_u \quad \text{(for clayey soils)} \qquad (1)$$

$$E' = 2\ N \quad \text{(in MPa for sandy soils)} \qquad (2)$$

in which S_u = undrained shearing strength, and N = blow counts in standard penetration tests. The Mohr-Coulomb Model was adopted to simulate the stress-strain behavior of soils.

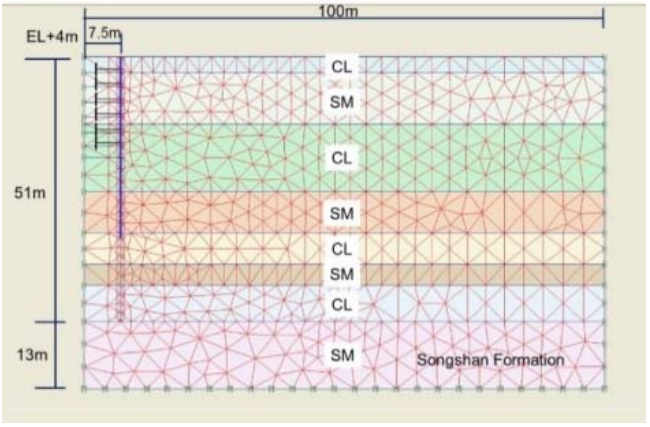

Figure 19 Finite element mesh for the Crossover next to G17 Station

The deepest borehole was sunk to a depth of 51m and it is remarked that the soils below this depth were SM. In the analyses, an E' value of 75 MPa was assumed for the material below this depth and the rigid base was assumed at a depth of 65m which was estimated based on local geology. The water pressures acting on the outer face of the diaphragm wall are shown in Figure 20. Inside the pit, the water level was assumed to be at a depth of 1m below the bottom of the excavation in each stage. The diaphragm walls were simulated by plate elements and an E value of 25,000 MPa was adopted for concrete with a fc value of 280 kg/cm2.

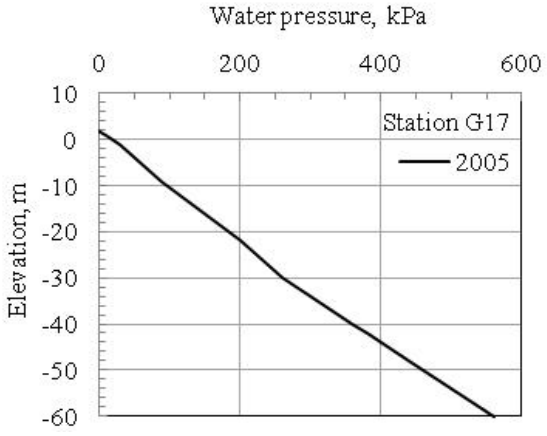

Figure 20 Groundwater pressures on the outer face of diaphragm wall

Table 4 Soil properties and soil parameters adopted (MAA 2005)

Depth (m)	Soil Type	γ_t (kN/m^3)	N (blows)	S_u (kPa)	c' (kPa)	Φ' (deg)	E' (MN/m^2)	Poisson's Ratio, υ'
0-3	CL	18.8	4	25	0	30	12.5	0.35
3-13	SM	19.2	8	-	0	32	20.0	0.30
13-26	CL	18.6	6	65	0	32	32.5	0.35
26-34	SM	19.4	13	-	0	32	32.5	0.30
34-40	CL	18.9	13	110	0	32	55.0	0.35
40-44	CL	19.7	21	-	0	32	52.5	0.30
44-51	SM	19.9	20	145	0	32	72.5	0.35

The EI (I = moment of inertia) and EA (A = sectional area) values of the diaphragm walls were reduced by 30%, giving a value of 1,464 MN*m for the former and 17,570 MN/m for the later, following the normal practice to account for the influence of tremieing and degradation of concrete during excavation. The structural properties of the struts are shown in Table 5. Of the 4 inclinometers installed in this section of the crossover, SID-2 and SID-3 gave the largest wall deflections, refer to Figure 18. The first set of readings of SID-3 was taken after the struts at the first level had been preloaded, therefore, is inappropriate for discussion.

Table 5 Stiffness of struts adopted in numerical analyses

Level	Members	Sectional Area (cm^2)	Stiffness, AE/S (MN/m)
1	1H350x350x12x19	1 x 173.9	891
2, 3	1H400x400x13x21	1 x 218.7	1121
4	1H428x407x20x35	1 x 360.7	1849
5, 6	1H414x405x18x28	1 x 295.4	1514
Note: Spacing between struts = 4m			

The wall deflections obtained from the analyses are compared with the readings obtained by Inclinometer SID-2 in Figure 21. The deflections obtained from the numerical analyses for the 1st stage of excavation were in a very good agreement with the inclinometer readings. However, large outward movements were calculated for the 2nd stage of excavation, refer to Figure 22(a), presumably because of the use of Mohr-Coulomb Model which much under-estimates the soil moduli in the early stages of excavation. Secondly, the preloads are line load applied to all the struts at the same level simultaneously in two-dimensional numerical analyses; while in reality, struts were preloaded individually, one by one. Each time a strut was preloaded, the load was essentially a point load resisted by the entire wall and the wall movement would thus be smaller than what would be if all the struts at the same level were preloaded simultaneously. Wall movements due to preloading of neighbouring struts would be small because the loads in the struts which had already been preloaded were not sustaining.

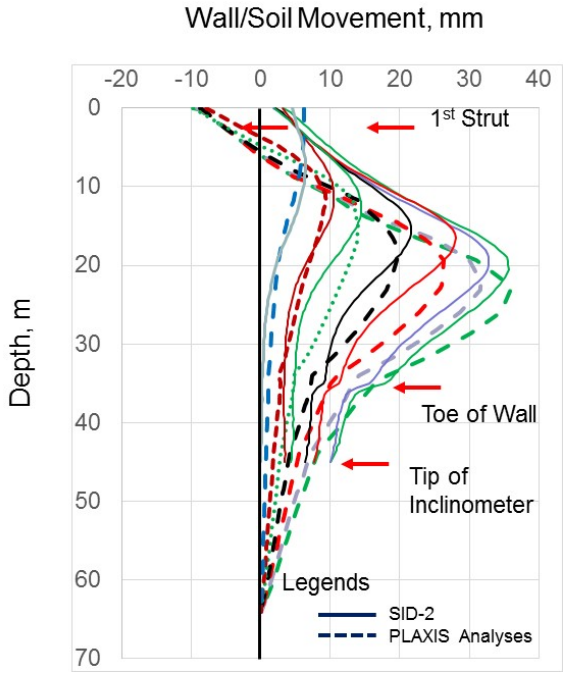

Figure 21 Comparison of computed wall deflections with inclinometer readings

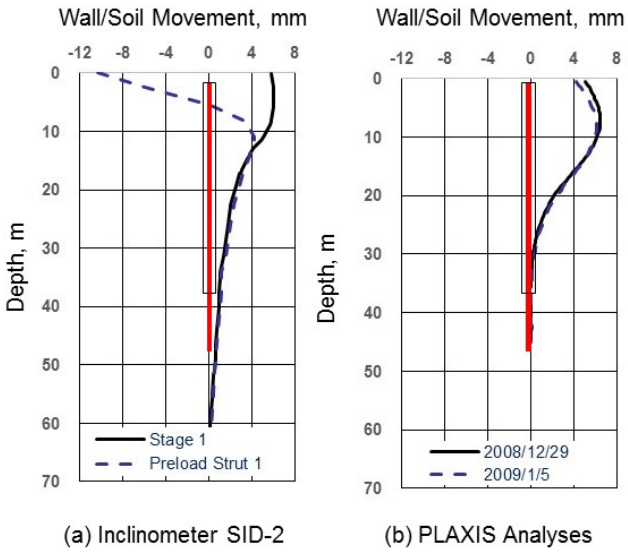

Figure 22 Influences of preloading the strut at the first level on wall deflections

4.3 Effects of Preloading of Struts

The strut at the first level at the location of SID-2 was preloaded to 72.5 tons (the average of 2 readings, refer to Figure 23) on 1 January 2009 and, as depicted in Figure 22(b), the inclinometer readings taken on 5 January indicated that the wall had hardly moved as compared to those taken on 29 December 2008. On the other hand, large outward wall deflections were computed by using PLAXIS. The drastic difference between the two scenarios certainly deserves further investigation.

Figure 23 shows the fact that the strut load dropped to nearly a half in a few days subsequent to preloading presumably due to preloading of neighbouring struts. This residual load can be considered as effective load in all the struts at the first level and should be the load to be adopted in numerical analyses. However, this reduction appears to be applicable to the first level only. As depicted in Figure 24, strut loads at the second level did not drop much after preloading.

The computed wall deflections with the preloads at the first level reduced by 50% are compared with the inclinometer readings in Figure 25. As can be noted, the outward movements shown in Figure 21 has been much reduced and the computed wall deflections agree better with the inclinometer readings. However, the improvement is limited to shallow depths and the maximum wall deflection in each stage of excavation is unaffected.

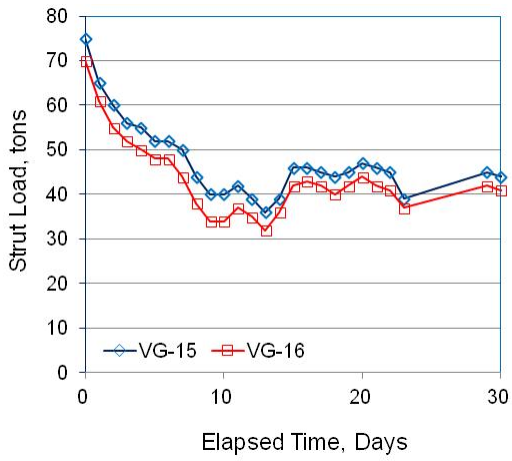

Figure 23 Strut loads at the first level subsequent to preloading

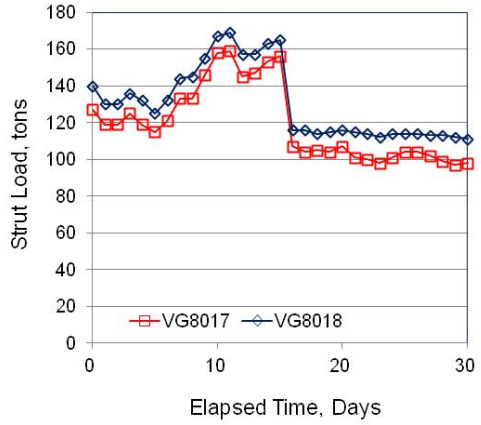

Figure 24 Strut loads at the second level subsequent to preloading

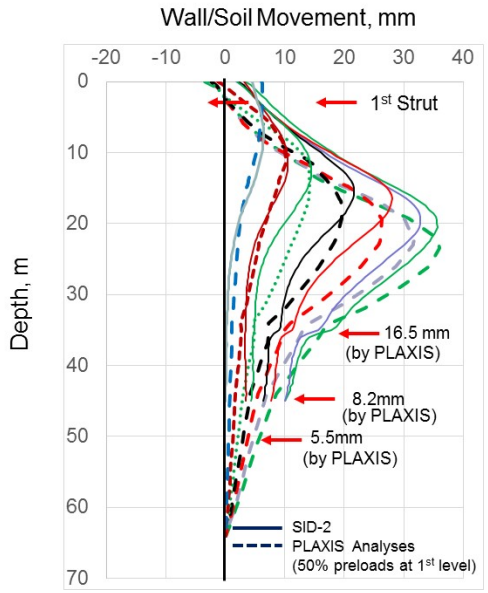

Figure 25 Comparison of wall deflections for the benchmark case with inclinometer readings

The case shown in Figure 25 is considered as the "benchmark case" for parametric studies. For academic interest, analyses have also been carried out for the case with preloads in all stages of excavation ignored and the results are shown in Figure 26. As can be noted that the shapes of the deflection profiles computed agree very well with those obtained based on the inclinometer readings, however, the maximum wall deflection increases from 36mm to 44.5mm at the end of the excavation.

4.4 Movements at Diaphragm Wall Toes

The computed movements at the first strut level, toe of diaphragm wall and tip of inclinometer are given in Table 6. It is readily apparent, by comparing Figure 25 with Figure 18, that the computed movements at the diaphragm wall toe and at the tip of inclinometer well agree with those estimated based on the readings of SID-2.

What is of great significance is the fact that the rational given in Section 4.1 for correcting the movements of the diaphragm wall and at the tip of inclinometer based on the movements at the first strut level subsequent to preloading was confirmed by the analyses. As can be noted, the movement at the 1st strut level increased from 1.53mm after preloading of the strut (inward) to 2.59mm at the end of Stage 2 excavation, and then dropped to 0.17mm at the end of the final excavation. These increments and decrements agree well with those deduced from strut loads in Section 4.1; and movements of such magnitudes are indeed negligible in comparison with the large movements at the diaphragm wall toes and at the tips of inclinometers; and inclinometer readings can indeed be calibrated accordingly for practical purposes.

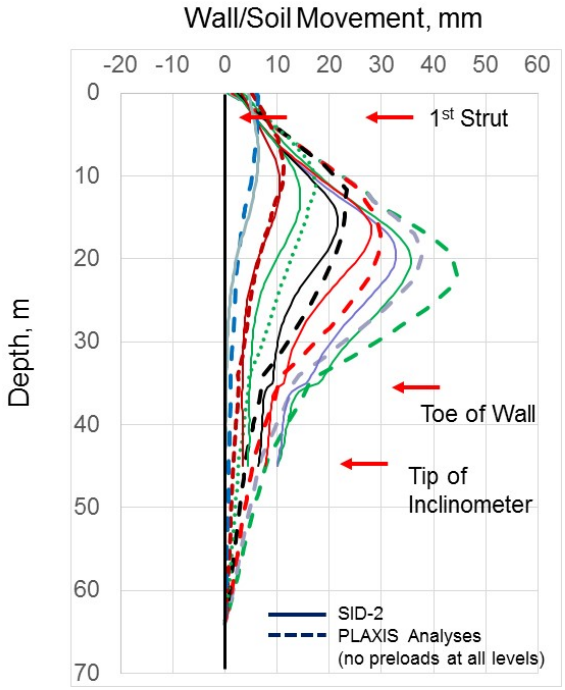

Figure 26 Comparison of results of numerical analyses for the case without preloads at all levels with inclinometer readings

Table 6 Movements computed in numerical analyses for the benchmark case

	Movement, mm		
	1st Strut Level	Toe of Wall	Inclinometer Tip
Stage 1 Excavation	6.26	1.09	0.76
Preload 1st Strut	1.53	1.20	0.82
Stage 2 Excavation	2.59	2.80	1.63
Preload 2nd Strut	0.94	2.92	1.70
Stage 3 Excavation	0.47	4.54	2.79
Preload 3rd Strut	0.62	4.89	2.65
Stage 4 Excavation	0.27	7.39	3.85
Preload 4th Strut	0.43	7.10	4.06
Stage 5 Excavation	0.25	10.31	5.05
Preload 5th Strut	0.33	10.42	5.09
Stage 6 Excavation	0.23	13.06	6.89
Preload 6th Strut	0.23	13.33	6.36
Stage 7 Excavation	0.17	16.50	8.15
Note: plus values for inward movements and minus values for outward movements			

Similar numerical analyses have been performed for Shandao Temple Station (BL8 Station), refer to Figure 1 (Location 6) for location and Figure 27 for soil profile, and the results are available in Hwang et al. (2012). Based on the results obtained, Hwang et al. 2016 proposed to adopt Figure 28 to estimate the toe movements of walls of 1m in thickness for excavations of various widths. Accordingly, a toe movement of 15mm, roughly, was obtained for the case of interest, i.e., with a width of excavation of 15m and a depth of excavation of 18.9m, by interpolation. Since the diaphragm wall at BL8 Station was 30.5m in length while the wall for the case of interest, i.e., excavation at G17, was 35m, toe movements have to be adjusted by proportioning using Figure 29 which was proposed in

Hwang et al. (2016) based on the inclinometer readings obtained at three sites (Hwang et al. 2007b). The ratios of toe movements are 2/3/6 for walls of 35m/30m/24m in length. The toe movement for the case of interest is reduced from 15mm to 10mm accordingly.

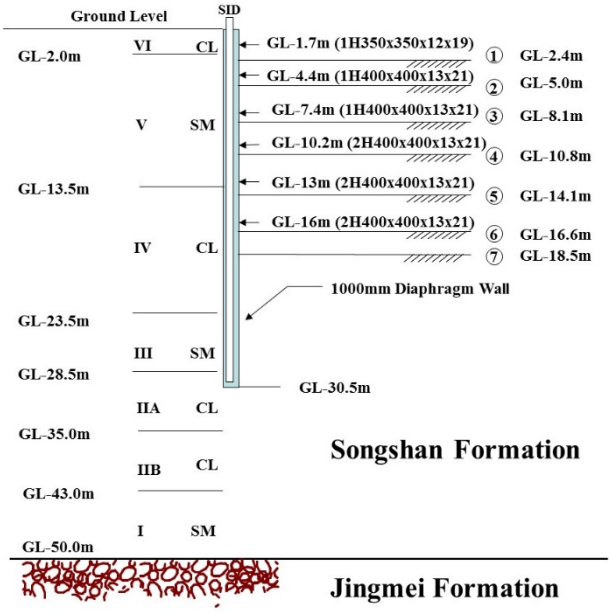

Figure 27 Soil profile at Shandao Temple Station (BL8 Station)

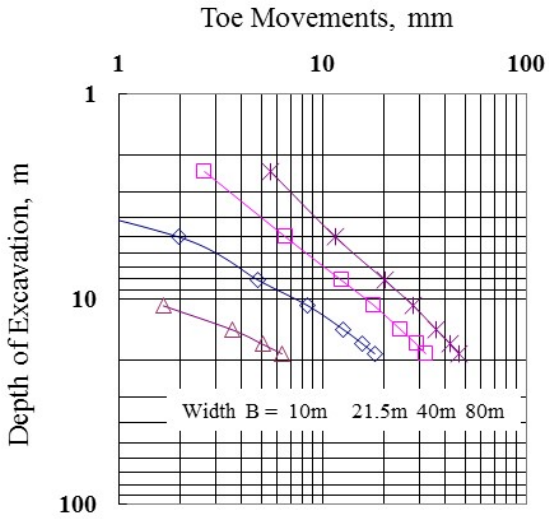

Figure 28 Toe movements of walls of 1m in thickness and 30m in length for various width of excavations in soft deposits with a thickness of 50m

Furthermore, Figures 28 and 29 are applicable to excavations in soft deposits of 50m in thickness, refer to Figure 27 while the thickness of soft deposits is 65m, refer to Figure 19. As can be noted from Figure 25, the computed movement at a depth of 50m is 5.5mm. The estimated toe movement for the case of interest would then be 10mm + 5.5mm = 15.5mm which is about the same as that computed in PLAXIS analyses, refer to Figure 25.

This exercise confirms the validity of the procedures proposed by Hwang et al. (2016) for estimating toe movements. It also illustrates the importance of width of excavation, wall length and the thickness of soft deposits on toe movements.

The thickness of wall certainly is a dominating factor affecting toe movements. The discussion, however, is beyond the scope of this paper.

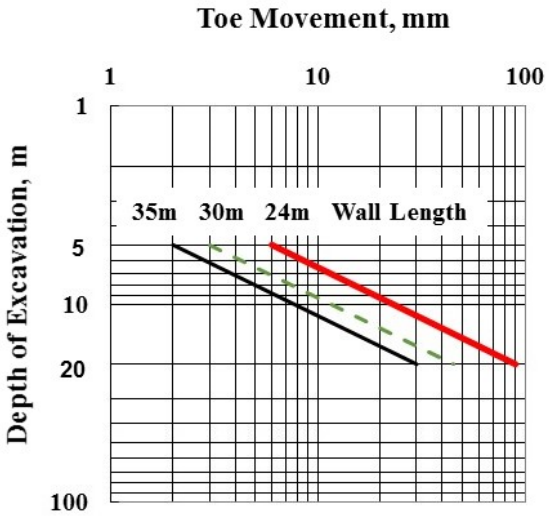

Figure 29 Relative Toe movements for various lengths of diaphragm walls with a thickness of 1m

5. WALL DEFLECTION PATHS AND REFERENCE ENVELOPES

To evaluate the performance of excavations, the concept of wall deflection path was first proposed by Moh and Hwang (2005) and subsequently adopted in Hwang and Moh (2007) and Hwang, et al. (2006; 2007a; 2012). A wall deflection path is the plot of the maximum wall deflections obtained in various stages of excavation versus the depths of excavation in a log-log scale to show how wall deflections develop as excavation proceeds. Figure 30 shows the wall deflection paths for the case of interest based on the inclinometer readings which have been corrected to account for the movements at the tips of inclinometers.

In congested city areas, there are most likely high-rise buildings with deep basements and/or large infrastructures such as underpasses, drainage boxes and common ducts, etc., alongside new excavations. This is particularly true for excavations for metro stations and cut-and-cover tunnels, which are normally constructed underneath major streets. These basements and/or large infrastructures normally have retaining walls left in-place after the completion of construction, hence, wall deflections in new excavations are very likely to be reduced as a result. Furthermore, there are always entrances, ventilation shaft, etc. structurally connected to the station walls and, therefore, the rigidity of the walls is much increased and wall deflections are much reduced. Some of the inclinometers may locate close to corners and their movements are restrained by the side walls.

The case of interest is a typical example to illustrate the importance of all these influencing factors. As can be noted from Figure 15, there are buildings with various heights on both sides of the crossover. Inclinometer SID-1 was located next to a short side of a working shaft and the wall deflections at this location were restrained by the two diaphragm walls in the perpendicular direction. Inclinometer SID-6 was located at where the station connects to a joint development and the wall has a Z-shape. Since all these factors are not considered in back analyses which are normally carried out by two-dimensional numerical analyses, Figure 19 for example, comparison of the results obtained in back analyses with the observed performance of the walls often leads to mis-leading conclusions.

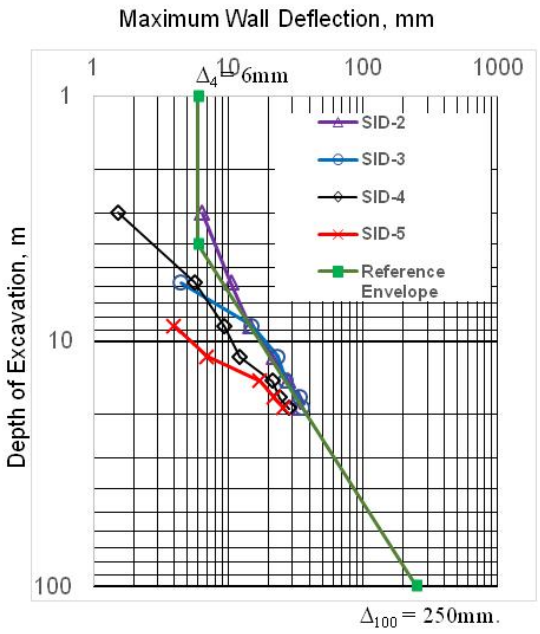

Figure 30 Wall deflection paths and reference envelope for the crossover

The drastic differences between the wall deflection paths shown in Figure 30 fully demonstrate the ambiguity faced in back analyses. Different results will be obtained if a different set of inclinometer readings is selected to match the results of numerical analyses. To establish a consistent methodology for back analyses, Moh and Hwang (2005) suggested to take the upper envelope of the wall deflection paths as "reference envelope" to compare with the results of conventional two dimensional numerical analyses which are usually conducted for excavations in green field without structures or utilities in the vicinity. This suggestion was based on the belief that wall deflections are likely to be reduced by many factors and the upper envelope of wall deflection paths will be closer to what will be obtained in numerical analyses carried out for excavations in green field. For convenience, reference envelopes are defined by the wall deflections for a depth of excavation of 4m, i.e., Δ_4 and the wall deflection projected to a depth of excavation of 100m, i.e., Δ_{100}. Accordingly, the reference envelope for the case of interest can be expressed as Δ_4 = 6mm and Δ_{100} = 250mm as depicted in Figure 30.

Excavation and preloading of struts at excavation sites are never carried out in the ways specified in designs. They are carried out in a rather unpredictable sequence as there are site constraints and project progress to be considered, and coordination among subcontractors sometimes is difficult. Over-excavation occurs rather frequently and delay in strutting is quite common. For these reasons, the data for shallow excavation are erratic and only the data for excavations exceeding 10m in depth should be considered in establishing wall deflection paths and reference envelopes as suggested in literature (Moh and Hwang 2005; Hwang et al. 2006, 2007a, 2007b).

For numerical analyses, as discussed in Section 4.3, wall deflections at shallow depths are likely to be affected by how the preloads at the first and the second levels are handled. Therefore the data for shallow excavations should also be ignored. After all, shallow excavations are not of interest. The wall deflection path obtained by PLAXIS analyses is given in Figure 31 and can be defined by Δ_4 = 6mm and Δ_{100} = 250mm. This wall deflection path is identical to the reference envelope given in Figure 30. The agreement is rather accidental as Equations 1 and 2 were adopted without deliberate efforts for the results of analyses to match the observation.

To illustrate how the concept of wall deflection path and reference envelope can be applied in evaluation the influences of various factors on the performance of diaphragm walls, numerical analyses were conducted for different thicknesses of walls and the results are depicted in Figure 32. This figure together with Figure 31 show that the Δ_4 values (i.e., 6mm) are unaffected by the thickness of diaphragm wall while the Δ_{100} values increase from 180mm to 250mm and to 320mm as the thickness of wall decreases from 1.5m to 1m and to 0.6m. For a depth of excavation of 20m, the maximum wall deflections will be 32.8mm, 38.7mm and 43.8mm, respectively.

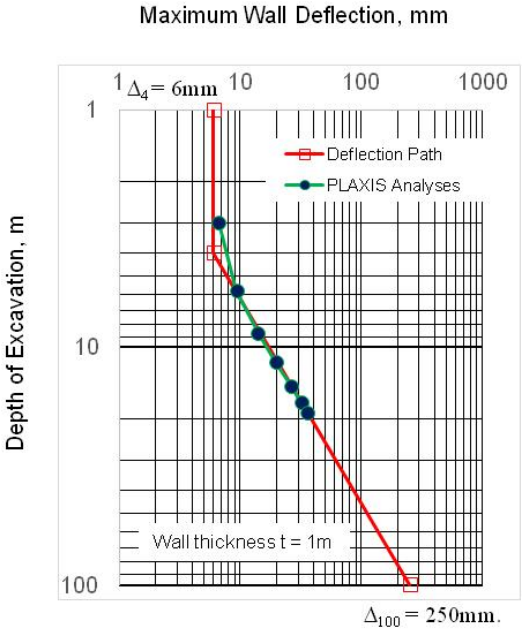

Figure 31 Wall deflection path obtained by PLAXIS analyses for the benchmark case

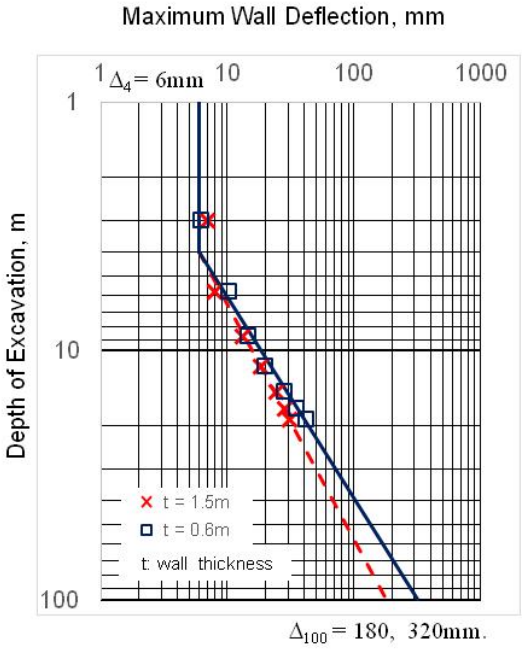

Figure 32 Influences of thickness of diaphragm wall on wall deflection paths obtained by PLAXIS analyses

The wall deflection path for the case without preloads at all strut levels, refer to Figure 26, is depicted in Figure 33. As far as the maximum wall deflections are concerned, the influence of preloads is similar to the influence of wall thickness. As can be noted, preloads does increase the rigidity of the retaining system.

Analyses were also performed for different widths of excavation and the results are given in Figure 34. As can be noted that the Δ_4 values are more or less proportional to the width of excavation. This is one of the reasons for Inclinometers SID-6 and SID-7, refer to Figure 15, to be excluded from this study. The fact that wall deflection paths for different widths of excavation tend to give the same Δ_{100} values is consistent with the finding given in Hwang et al. (2012) and Hsiung et al. (2016)..

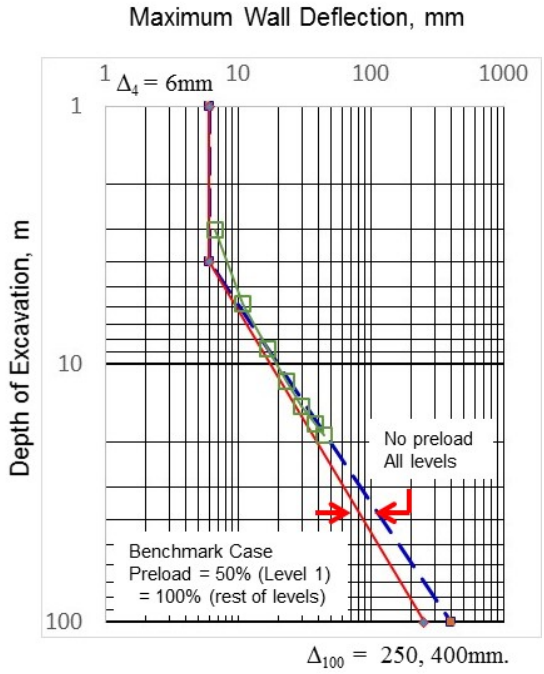

Figure 33 Influences of Preloading of struts on wall deflection paths obtained by PLAXIS analyses

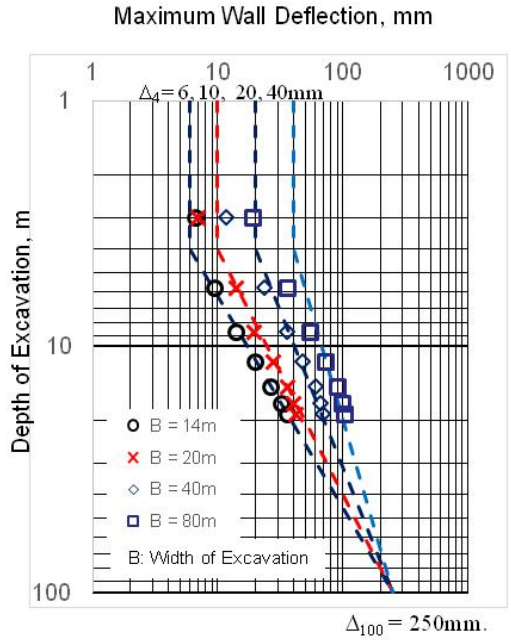

Figure 34 Influences of width of excavation on wall deflection paths obtained by PLAXIS analyses

This above discussions demonstrate how easy it is to quantify the influences of various parameters on wall deflections by adopting the concept of wall deflection path and reference envelope.

6. CONCLUSIONS

The foregoing discussions lead to the following conclusions:

(1) The presence of the Jingmei Formation is a unique feature of the Taipei Basin and the groundwater pressure in the Jingmei Formation is one of the most important factors to be considered for deep excavations. Deep excavations have been benefited by the lowering of groundwater pressures in the Jingmei Formation in the 1970's and the recovery of the pressures since 1980's makes deep excavation challenging.

(2) Inclinometer readings must been calibrated to account for the movements at the tips. In most cases it is appropriate to assume that the joints between the struts at the first level and diaphragm walls will not move once these struts are preloaded so readings can be calibrated accordingly.

(3) The preloads in the struts at the first level shall be properly reduced in numerical analyses to account for the reduction due to preloading of neighboring struts. In the case of interest, a reduction factor of 50% was found appropriate.

(4) Wall deflection path and reference envelope are useful tools in evaluating the influences of various factors on movements of diaphragm walls.

7. ACKOWLEDGEMENTS

The authors are grateful to the Department of Rapid Transit Department of Taipei City Government for the opportunity of serving as Detailed Design Consultant of Design Lot DG166 and to RSEA Engineering Corporation for the opportunity of providing consulting services for the construction of the Turnout. The instrument readings presented herein were obtained from Maeda Corporation and the results of numerical analyses were provided by Mr. Wong Lup Wong. The authors wish to express sincere appreciation to their valuable supports.

8. REFERENCES

Chin, C.T., Crooks, A.J.H., and Moh, Z.C. (1994). "Geotechnical properties of the cohesive Sungshan deposits, Taipei", Geotechnical Engineering Journal, Southeast Asian Geotechnical Society, 77-103

Chin, C.T. (1997) Groundwater control during the construction of Taipei MRT. Proc., 14th Int'l. Conf. on Soil Mech. and Foundation Engineering., Hamburg, Germany.

Chin, C.T. and Liu, C.C. (1997) Volumetric and undrained behaviors of Taipei silty clay. J. of the Chinese Inst. of Civil and Hydraulic Engineering, 9(4): 665-678. (in Chinese)

DORTS (2010) Turnout structure and cross-river tunnels for the Xinzhuang Line, MRT Constructions, no. 41, Department of Rapid Transit Systems, Taipei City Government, Taipei, Taiwan

Hu, I.C., Chin, C.T., and Liu, C.J. (1996) Review of the geotechnical characteristics of the soil deposits in Taipei. Sino-Geotechnics, 54: 5-14. (in Chinese)

Hsiung, B. C., Dan, D. S. and Lum, C. W.(2016) Evaluation of performance of diaphragm walls by wall deflection paths for deep excavations in Central Ha Noi, Geotechnical Engineering, J. of the SEAGS & AGSSEA, v.47, no. 1, March, ISSN 0046-5828

Hwang, R. N., Moh, Z. C., Yang, G. R., Fan, C. B., Chao, C. L. and Wong, R. K. (1998). Ground Freezing for Repairing a Damaged Tunnel, Special Lecture, Proceedings of 13th Southeast Asian Geotechnical Conference, 16~20, November, Taipei, Taiwan, pp. 16-20

Hwang, R. N., Moh, Z. C. and Kao, C. C. (2006). "Design and construction of deep excavations in Taiwan", Seminar on "The State-of-the-Practice of Geotechnical Engineering in Taiwan and Hong Kong , Hong Kong, 20 January

Hwang R. N. and Moh, Z. C. (2007) Deflections paths and reference envelopes for diaphragm walls in the Taipei Basin, J. of GeoEngineering , Taiwan Geotechnical Society, v2, no .1, April, Taipei, Taiwan, 1~12

Hwang, R. N., Moh, Z. C. and Kao, C. C. (2007a). "Reference envelopes for evaluating performance of diaphragm walls", 13th Asian Regional Conference, December, Kolkata, India, pp. 505~508

Hwang, R. N., Moh, Z. C. and Wang, C. H. (2007b). "Toe movements of diaphragm walls and correction of inclinometer readings", J. of GeoEngineering, Taiwan Geotechnical Society, Taipei, Taiwan, v2, no. 2, August, pp. 61~72

Hwang, R., Lee, T. Y., Chou, C. R., and Su, T. C. (2012) Evaluation of performance of diaphragm walls by wall deflection paths, J. of GeoEngineering, v2, no. 1, April, Taiwan Geotechnical Society, Taipei, Taiwan 1~12

Hwang, R. N., Moh, Z. C., and Hu, I. C. (2013) Effects of Consolidation and specimen disturbance on strengths of Taipei Clays, J. Geotechnical Engineering, v44, no. 1, March, Southeast Asian Geotechnical Society & Association of Geotechnical Societies in Southeast Asia, Bangkok, 9~18

Hwang, R. N., Wang, C. H., Chou, C. R. and Wong, L. W. (2016) Deep excavations in Taipei Basin and performance of diaphragm walls, Geotechnical Engineering, J. of the SEAGS & AGSSEA, v.47, no. 2, June, ISSN 0046-5828

Ladd, C.C. and Foote, R. (1974). "A new design procedure for stability of soft clays". J. of the Geotechnical Engineering Division. ASCE, Vol. 100, No. GT7. pp. 763-786.

Lee, S.H. (1996). "Engineering Geological Zonation for the Taipei City", Sino-Geotechnics, vol. 54, April (in Chinese)

Lin, L. S., Ju, D. H. and Hwang, R. N. (1997). A case study of piping failure associated with shield tunnelling, Proceedings of 15th International No-Dig '97, November 26~28, Taipei, Taiwan, pp. 6B-1-1~6B-1-13

MAA (1987) Engineering properties of the soil deposits in the Taipei Basin. Report No. 85043, Ret-Ser Engineering Agency and Taipei Public Works Department, Taipei. (in Chinese)

MAA (2005) Design Summary, Construction Contract CG292, Songshan Line, submitted to Department of Rapid Transit Systems, Taipei City Government, by Moh and Associates, Inc., Taipei, Taiwan

MAA Group (2007) Engineering characteristics of Taipei Clay, MAA Group Consulting Engineers, Taipei, Taiwan

Moh, Z.C. and Ou, C.D. (1979) Engineering characteristics of Taipei silt. Proc. 6th Asian Regional Conf. on Soil Mech. and Found. Engineering, 1, Singapore, 155-158.

Moh, Z. C. and Hwang, R. N. (1997) Geotechnical problems related to design and construction of the Taipei Transit Systems, Proc., Keynote Speech, Professor Chin Fung Kee Memorial Lecture, September 6, Kuala Lumpur, Malaysia

Moh, Z. C., Ju, D. H. and Hwang, R. N. (1997). A small hole could become really big, Momentous Session, Proc., 14th Int. Conf. on Soil Mechanics and Foundation Engineering, September 6-12, Hamburg, Germany

Moh, Z. C. and Hwang, R. N. (2005). "Geotechnical Considerations in the Design and Construction of Subways in Urban Areas", Seminar on Recent Developments on Mitigation of Natural Disasters, Urban Transportation and Construction Industry, 30 November – 2 December, Jakarta Indonesia

Moh, Z. C. and Hwang, R. N. (2015) Challenges in recent underground construction in Taiwan, Proc., 15th Asian Regional Conference, November 9-13, Fukuoka, Japan

Ou, C. D., Li Y-G and Cheng, T-J (1983) The influence of distribution of ground water pressure on the foundation engineering in Taipei Basin, J. of the Chinese Institute of Civil and Hydraulic Engineering, vol. 10, no. 3, Nov. 1983, pp. 89-102 (in Chinese)

PLAXIS BV (2011). "Reference Manual", PLAXIS BV, Amsterdam, the Netherlands

Teng, L.S. , Wang, S.C., Chang, C.P., Hsu, C., Yuan, P.B., and Chen, P.Y. (1994) Stratigraphy of the Quaternary in the Taipei Basin. Procs., Joint Symposium on Taiwan Quaternary V and on Investigation of Subsurface Geology and Engineering Environment of Taipei Basin: 129-135. (in Chinese)

Teng, L.S, Yuan, P. B, Chen, P. Y. Peng, C H., Lai, T. C., Fei, L. Y. and Liu, H. C. (1999), Lithostratigraphy of Taipei Basin Deposits, Central Geological Survey, Special Issue, No. 11, pp. 41-66, Taiwan (in Chinese)

Teng, L. S., Liu, T. K., Chen, Y. G., Liew, P. M., Lee, C. T., Liu, H. C. and Peng, C. H. (2004) Influence of Tahan River Capture over the Taipei Basin, Geography Research, National Taiwan Normal University, No. 41, November, Taiwan (in Chinese)

WRPC (1976) Level survey of benchmark network of the Taipei Basin, Annual Report of Water and Resources Planning Commission (in Chinese)

Wu, C. M. (1968) Subsidence in Taipei Basin, Part II, J. of the Chinese Institute of Civil and Hydraulic Engineering, Taipei, Taiwan, v4, pp 53~81 (in Chinese)